Comparison between a Digital and an Analog Active Noise Control System for Headphones

Artur Zorzo, William D'Andrea Fonseca, Paulo Mareze and Eric Brandao
Department of Acoustical Engineering, Federal University of Santa Maria, RS, Brazil.

Summary
Active noise control can be a powerful tool when dealing with problematic low-frequency tones or general broadband noise. The primary goal of this paper is to discuss design methods, analyze their performance in measurements and to compare analog and digital Active Noise Control (ANC) systems for headphones. The systems were implemented for an AKG K44 headphone. The algorithm used for the digital system was the FXLMS (Filtered Least Mean Squared), which is a variation of the Least Mean Square algorithm (LMS). As for the analog version, filtering and inversion circuits were designed based on a precision operational amplifier. The same microphone preamplifier was used in both systems. The performances were measured using a head and torso simulator (HATS) and the external noise was generated by a dodecahedral omnidirectional sound source (in a reverberation room). Some results were impaired by the poor coupling between the headphone and the pinna of the HATS utilized. For this reason, the complete measurement set was carried out with and without the artificial pinna (outcomes are discussed throughout this work). Although the digital system was designed to attenuate broadband noise, great results were achieved for both: broadband and tonal noise. The results for the tonal noise were not as expressive in the analog system as they were for the digital version. Nevertheless, similar results were accomplished for the broadband noise. For this paper, only a few values of the algorithm's convergence parameters were tested. Therefore, better results may still be obtained for the digital system with the correct adjustment of these values. Moreover, it is possible to improve the sound attenuation (for both systems) with a more refined design for the preamplifier and analog filters.

PACS no. xx.xx.Nn, xx.xx.Nn

1. Introduction

Active Noise Control (ANC) can be a useful tool when reducing excessive and/or undesired Sound Pressure Levels (SPL). This technique is based upon the wave superposition principle, and it works by generating an anti-noise[1] that cancels the primary noise when they are added (in the same sound field) [1].

Passive noise control methods, like porous materials, barriers and enclosures usually are not able to reduce significantly SPL at lower frequencies, unless they are very large and bulky (which may lead to impractical implementation due to space limitations. On the other hand, according to Kuo and Morgan [2], ANC works mainly in the low-frequency range. This fact arises from the difficulty of adjusting the anti-noise's phase for high frequencies.

The application of this method in headphones has been already used in the field of aviation, specifically in communication devices used by pilots, to ensure good communication even with loud wind and engine noises. Furthermore, in the past few years, several headphones designed for audio and music have been developed with this ANC system. The goal in this situation is to make possible listening to songs in good quality even in loud environments such as train stations as well as airports.

The main purpose of this study is to demonstrate two feedback active noise control system designs: analog and digital. Accordingly, the evaluation and comparison of performances for tonal and broadband noise attenuation (in the frequency domain) are discussed.

2. Feedback Active Noise Control

According to Elliot and Nelson [1], one of the most successfully use of feedback ANC control has been applied to the design of broadband noise control systems for headphones. A feedback control system, firstly described by Olson and May [3], is based upon an

[1] For example, if a sine is considered, the anti-noise would be another sine with a 180° phase shift.

error microphone in the position where the reduction is desired and a loudspeaker close to the microphone. A diagram of such configuration can be observed in Figure 1. The controller purpose is to generate a signal to the loudspeaker that minimizes the error captured by the microphone.

The major problem of this configuration is that the phase distortions due to the circuitry, acoustic path between microphone and loudspeaker and the loudspeaker itself can impair the performance of the controller and even generate positive feedback at higher frequencies (if the phase delays diverge too much from the 180 degrees goal). Thus, these secondary systems have to be accounted for and the distance between the microphone and the loudspeaker (source-receiver) should be small as possible.

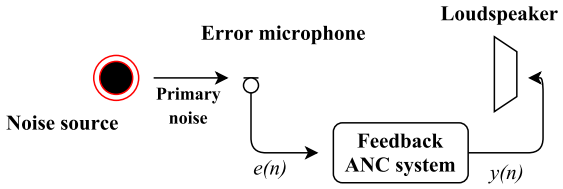

Figure 1: Basic model of a feedback active noise control system (adapted from [2]).

3. Controller Designs

In this section, both control systems, analog and digital, will be described, regarding the basic principles and algorithms. In the next section, the circuit diagrams and hardware will be presented.

3.1. Analog System

The analog active noise control system built for this project was based on amplification, filtering and inversion circuits.

The amplification stage was the same for both designs, analog and digital, and will be further explored in the next Section. The filtering stage is necessary to prevent high frequencies to be amplified and generate positive feedback. The frequency where the positive feedback starts to occur depends on the group delay caused by the distance between the microphone and loudspeaker, as well as to the phase distortions of the circuits and loudspeaker.

For this design, to avoid this effect, a first-order low-pass filter was implemented with a cut-off frequency of 800 Hz. The filtering and inversion circuits will also be shown in Section 4.

3.2. Digital System

This section will introduce the theories and the necessary steps regarding the algorithm used.

3.2.1. FXLMS Algorithm

The algorithm used for the digital part of this research was the FXLMS (Filtered Least Mean Squared), which is a variation of the Least Mean Square algorithm (LMS). The method is based on an adaptive finite impulse response (FIR) filter that varies its coefficients in order to minimize the square of the error measurement [2] (or to minimize the variance of error signal). The complete diagram of the algorithm can be observed in Figure 2.

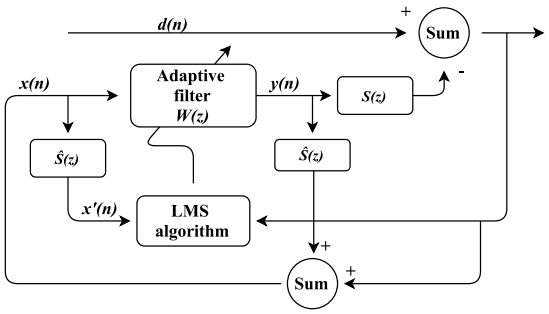

Figure 2: Diagram of the FXLMS algorithm (adapted from [2]).

The equations related to the filter and the adaptive algorithm will be shown throughout this section (further reading about LMS may be found in textbook by Clarkson [4]). Herein, vectors and matrices will be denoted by uppercase letters and scalar quantities denoted by lowercase letters. The FIR filter is defined as a vector $W(n)$ with L coefficients and the input vector $X(n)$ is defined as a vector of the same size, where $x(n)$ represent the current input value, $x(n-1)$ the immediately past input value and so on and so forth. The cited vectors can be denoted by

$$W(n) = [\, w_0(n)\ w_1(n)\ \cdots\ w_{L-1}(n) \,]\,, \tag{1}$$

and

$$X(n) = [\, x(n)\ x(n-1)\ \cdots\ x(n-L+1) \,]\,. \tag{2}$$

For each discrete value of time n, the error is given by the microphone's measurement.

The output of the filter can be computed as a real-time convolution (Equation 3) between the filter's impulse response ($\mathrm{IR}_{\mathrm{filter}}$) and the input vector (Equation 2). This convolution can also be expressed as the *vector product* of the transposed version of vector the $W(n)$ and the input vector $X(n)$. Therefore,

$$Y(n) = \sum_{i=0}^{L-1} w_i(n)\, x(n-i) = W^T(n)\, X(n)\,. \tag{3}$$

There is a significant amount of phase and amplitude distortion between the exit and the input of the controller, called secondary path. These distortions are given by the loudspeaker, preamplifier, A/D and D/A converters, microphone and acoustic path between the

microphone and the loudspeaker. The sum of these systems' influence is denoted by $S(z)$ in the diagram of Figure 2 (the z is the derived by the use of Z-Transform [5]). If these distortions are not taken into account, the algorithm might become unstable. Therefore, an estimate of the secondary path ($\hat{S}(z)$) is performed to adjust the LMS[2] algorithm, hence, becoming FXLMS.

Equation 4 is responsible for updating the adaptive filter's coefficients in order to minimize the instantaneous squared error. The step size, represented by μ coordinates the rate in which the algorithm converges [6]. Accordingly,

$$w(n+1) = w(n) + \mu\, x'(n)\, e(n)\ , \tag{4}$$

where $e(n)$ is the error (considering a given threshold) and the $\{\cdot\}'$ indicates that a sample has passed through the $\hat{S}(z)$.

Since there is only one microphone, that measures the error, it is necessary to estimate the primary noise. This value can be computed by

$$x(n) \equiv \hat{d}(n) = e(n) + \sum_{m=0}^{M-1} \hat{s}_m\, y(n-m)\ . \tag{5}$$

Finally, the primary noise and the secondary path estimation are convoluted to generate the signal that is used to update the filter's coefficients. The convolution can be expressed by

$$x'(n) = \sum_{m=0}^{M-1} \hat{s}_m\, x(n-m)\ . \tag{6}$$

In practice, the algorithm is not able to reach the exactly the optimal solution. However, it achieves a fairly close point. The measure of how close the solution reaches the optimum is called misadjustment. If the step size is small, the algorithm will take longer to converge but the solution will get closer to the optimum, thus, the misadjustment value will be smaller. If μ is greater, the opposite event occurs, a fast convergence shall be expected, but after convergence, the solution will be far (or less close) to the desired value than with a small step size [7].

The shown algorithm is implemented in a streaming format. At each input sample converted by the controller, an output sample must be computed and emitted before the next input sample is gathered. Therefore, the sampling period must be higher than the time it takes the processor to compute the equations above (thereby decreasing the sampling frequency).

In this study, the sampling frequency was not set as a constant. At the codes loaded in the boards, each input sample is obtained as soon as the output sample is converted into analog value. Consequently, the sampling rate varies with the size of the filter. For this reason, there is a trade-off between filter size and sampling rate. If the filter size is too small, it might not be possible to achieve the necessary impulse response needed for a good performance. However, if the size of the filter is too wide, the sampling frequency, as well as the maximum frequency of analysis, is accordingly reduced. A continued study will consider a fixed sampling rate.

[2] The use of FXLMS was needed to overcome instabilities in the LMS approach.

3.2.2. Secondary Path Estimation

The secondary path estimation is obtained based on the *system identification technique*. According to Morgan and Kuo [6], the basic idea behind the system identification procedure is to construct a model based upon a measurement of the signal produced by the system. The diagram of the secondary path estimation can be consulted in Figure 3.

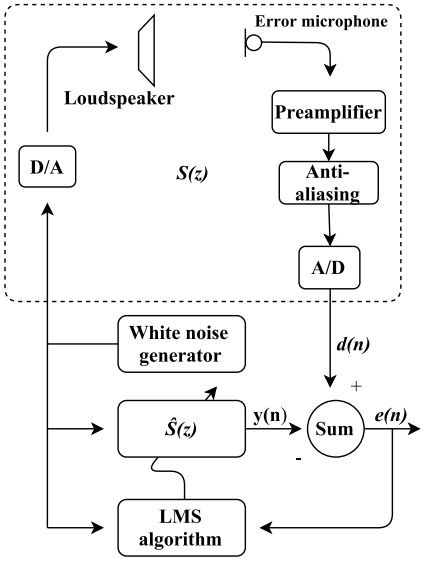

Figure 3: Secondary path estimation diagram (adapted from [2]).

An input signal $x(n)$, usually a broadband signal (such as a white noise), is generated by the processor and it serves as input to both adaptive filter and the secondary path.

The output of $S(z)$, expressed in the diagram by $d(n)$, and the output of the adaptive filter $\hat{S}(z)$, expressed by $y(n)$, are subtracted to generate an error signal $e(n)$. The error and the input signal are used by the minimization algorithm to adjust the filter to minimize the difference of the outputs.

When the error reaches its minimum (or the threshold), the IR of the adaptive filter is (in an optimum way) emulating the impulse response of $S(z)$.

4. Circuit Designs and Hardware

Both systems (analog and digital) were constructed with the same microphone capsule (JLI 61-A, observe Figure 4) [8] and preamplifier circuit [9]. The diagram

of the latter can be seen in Figure 5. This circuit is a modified version of Andy Collinson's design [10]. The original operational amplifier (opamp) was substituted by a precision, low-noise and rail-to-rail version (AD8606). This allows the amplifier system to be powered by low-voltage batteries.

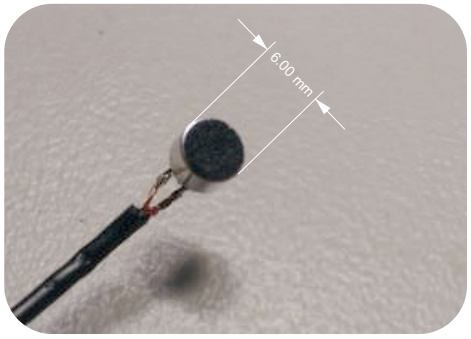

Figure 4: JLI-61A electret microphone capsule [8].

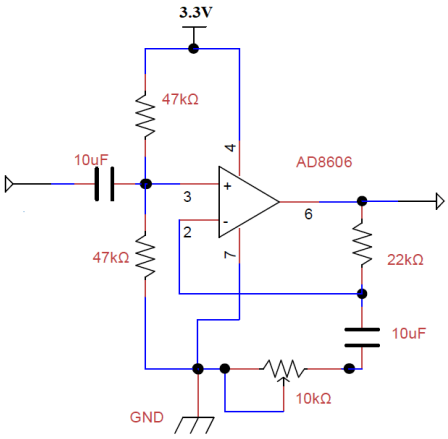

Figure 5: Preamplifier project for electret mic [9].

The microcontroller board operates with positive voltages. Thus, it is important to notice that the circuit adds a voltage offset (or bias), centered in half the power-supply voltage, to allow the signal to be amplified symmetrically.

Since all the circuits showed herein were meant to be independent and suitable for other projects, with different components and voltage supplies, this offset is withdrawn, by decoupling capacitors, and reset by the other circuits. This is an unnecessary step if they are going to be used for this sole purpose.

The circuit was simulated, and the frequency and phase response curves can be seen in Figure 6. The simulation was carried out with the highest possible gain (which depends upon the position of the potentiometer).

From the simulation results, it can be seen that the frequency response does not vary more than 3 decibels over a range of 20 Hz to 15000 Hz approximately. This frequency range is usually enough for most

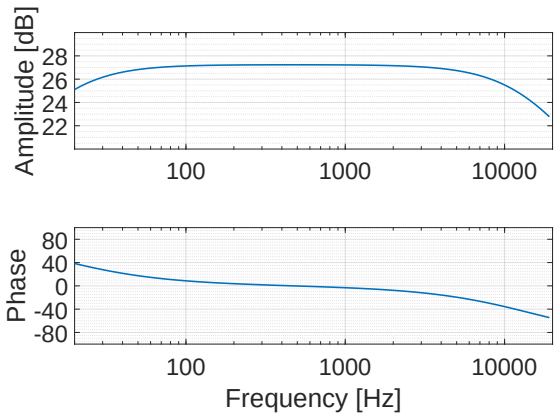

Figure 6: Simulation of the frequency and phase responses of the mic preamplifier.

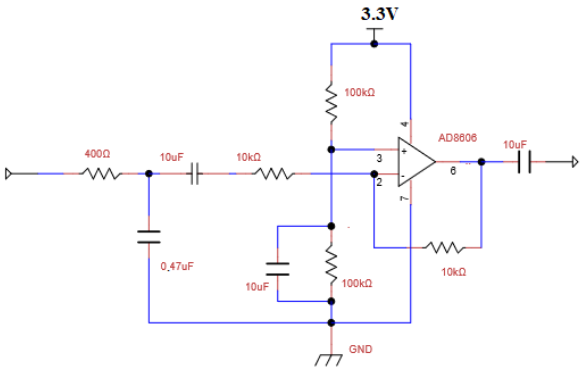

Figure 7: Filtering (RC low-pass) and inversion circuits.

audio and signal processing applications. However, if a larger frequency span is desired the circuit has to be redesigned.

The filtering and inversion circuit used in the analog noise canceling system can be seen in Figure 7. The filtering stage corresponds to a simple RC low-pass circuit with a cutoff frequency around 800 Hz. The inversion stage is carried out by the same opamp used for the preamplifier, but here without gain.

The FXLMS algorithm was implemented in a Teensy 3.6 board Figure 8. The board is based on a 32 bits ARM Cortex-M4 processor with floating point unit. The clock frequency of the microcontroller is 180 MHz, containing 12 bits A/D and D/A converters. More information about the board can be found in [11].

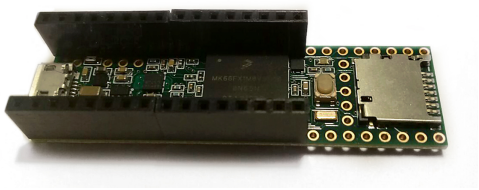

Figure 8: Teensy 3.6 microcontroller board.

Besides the preamplifier, some additional signal adjustment circuits were necessary to protect the hardware and to allow a correct sampling of the data.

Since the opamp was powered by the same operational voltage of the microcontroller, there was no need to design protection circuits for the inputs. However, the signal had to gain a voltage offset of half the operation voltage to guarantee the correct sampling, since the controller cannot sample negative voltages. Moreover, an anti-aliasing filter [5, 12] also had to be built to ensure that the high frequencies would not interfere in the system performance. The offset and anti-aliasing circuits can be observed in Figure 9.

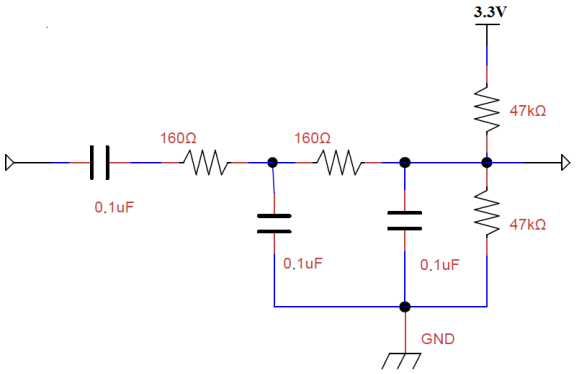

Figure 9: Anti-aliasing filter and offset adjustment circuit.

Small loudspeakers (or headphones), in general, have low impedance value [13]. Thus, if the outputs of the controller are connected directly to loudspeakers or headphone, the current drawn will be too much to the output ports, being enough to damage them.

A solution for this problem is to connect a voltage buffer to the output of the controller. With this configuration, the necessary current to power the speakers will be drawn directly from the power source. A voltage buffer specifically designed to power headphones can be seen in Figure 10. This circuit was proposed by Analog Devices (AD). The complete description of the AD8606 and other application notes can be consulted in [14].

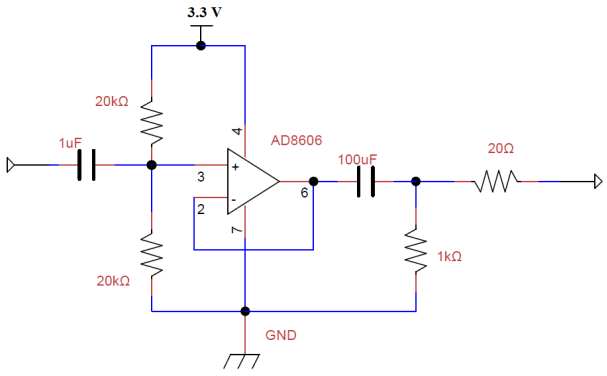

Figure 10: Headphone driver circuit (using a voltage buffer with AD8606 [14]).

5. Measurement Methodology

The performance measurements utilized the Head and Torso Simulator (HATS) Type 4128 from B&K [15]. The experiment was carried out inside a reverberation chamber with an omnidirectional sound source and LAN-XI as data acquisition system (see Figure 11). The signals tested were white noise (flat spectrum) and a 500 Hz tonal noise.

Figure 11: Instrumentation used to obtain the performance measurements (reverberation chamber).

During the measurements, it was noticed that the HATS's ears were too large for the chosen headphone, and, subsequently, the coupling was unsatisfactory. The measurements were then carried out with and without the artificial ears, for comparison purposes. Later, it was possible to realize that the bad coupling has impaired the performance of the control system. Therefore, only the results measured without the artificial ears will be shown herein.

The headphone used throughout this experiment was the AKG K44 [16], its picture, frequency response (FRF) and noise insulation are depicted in Figure 13. The error microphone was the JLI-61A [8], its FRF is shown in Figure 12. It is important show the FRFs of the mic and the headphone, hence the results can be better understood. The microphone was placed next to the HATS's microphone and connected into the preamplifier circuit that was designed for the controller. The headphone was setup to the simulator and connected to the controller's output.

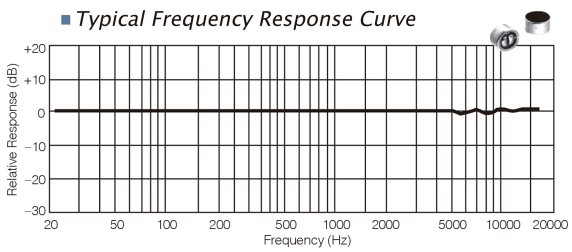

Figure 12: Electret JLI-61A typical microphone response (manufacturer measurement [8]).

(a) AKG K44 photo

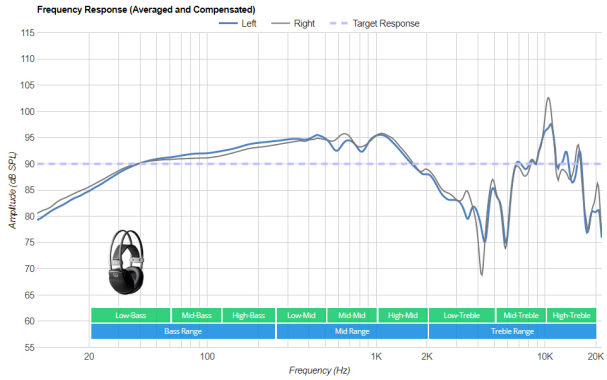

(b) FRF

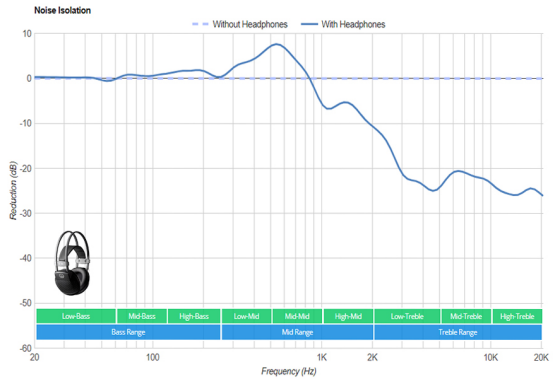

(c) Isolation

Figure 13: AKG K44 photo, frequency response (FRF) and noise insulation (rtings.com review [16]).

The designs were implemented only on the left side to reduce the research costs. Therefore, the results gathered represent just one ear of the HATS and the corresponding ANC system. The assumption made is that due to the diffuse field in the room, both sides would have similar results.

A variety of measurements were collected for both, white noise and the 500 Hz tone. For the digital algorithm, the filter length was varied for a given (fast converging) value of μ. The best results are shown in the following section.

The filter obtained in the off-line training step was also compared with the measurement of the headphone's transfer function multiplied by the frequency response of the simulated preamplifier (together with the anti-aliasing filter).

6. Results

The spectra of the results are limited to 2 kHz. That is, ANC is applied from the mid-bass to high-mid range of frequencies (as suggested by Kuo and Morgan [2]).

The attenuation results obtained with the analog system can be seen in Figures 14 and 15. For the tonal noise, the system was able to reduce about 10 decibels, considering the excitation frequency. However, some harmonics were amplified, especially the 1000 Hz tone. This result reveals the degree of non-linearity of the system, which is caused by distortions of the preamplifier and the loudspeaker. This effect is enhanced if the sound pressure level of the experiment is increased.

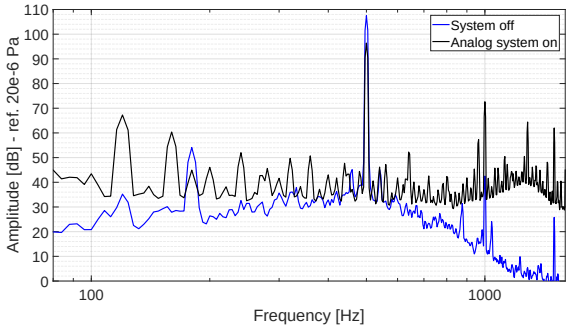

Figure 14: Performance of the analog ANC system for a 500 Hz tone.

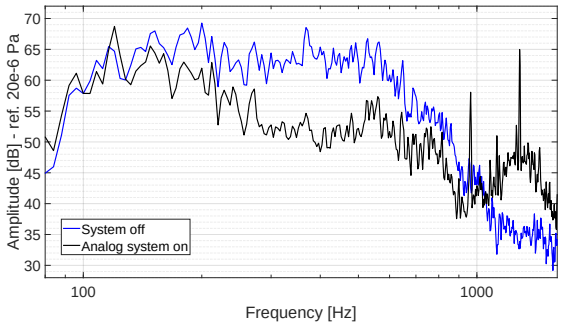

Figure 15: Performance of the analog ANC system for white noise (flat spectrum).

When the white noise acted as the noise to be reduced, the analog system was able to reduce notably the sound pressure levels in a frequency range of about 150 Hz to 900 Hz. However, as can be seen, above this frequency, several tones were amplified, reducing the overall performance of the system. Since the amplification was caused in discrete tones, the authors believe that this effect was again caused by the nonlinearities of the system and not due to positive feedback (although further studies must follow to assure the correct interpretation of the data).

The adaptive filtering theory described in Section 3, which is the basis of the digital system, relies upon the fact that the systems are linear. Therefore, the

attenuation provided by the algorithm may have been diminished by the degree of nonlinearities[3] occurred. However, good results were still obtained.

For the digital ANC, narrowband test, the 500 Hz tone has achieved the best result out of a filter length of 50 taps. The SPL reduction obtained was quite large, almost reaching a 40 dB reduction, as can be seen

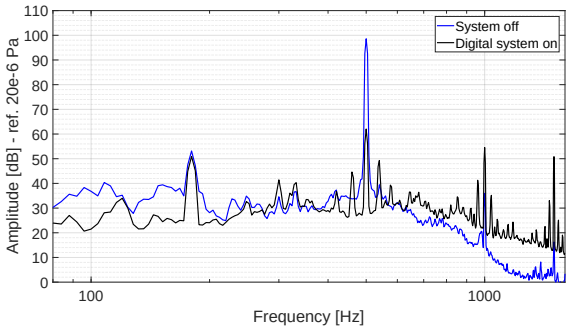

Figure 16: Performance of the digital ANC system with a 50 taps filter for a 500 Hz tone.

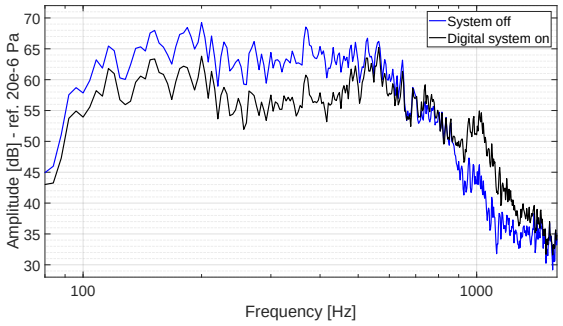

Figure 17: Performance of the digital ANC system with a 15 taps filter for white noise (flat spectrum).

in Figure 16. There were also some amplifications of harmonics, but the effect was less expressive than the previous results. The overall reduction was satisfactory.

The results obtained for the broadband noise were not as expressive as for the tonal noise, as per Figure 17. Nevertheless, some reduction was obtained for a frequency range from 50 Hz to 700 Hz. This result was obtained with a 15 taps filter. Although the small filter length might be limiting, a smaller length means a larger sampling rate. For the filters used in the tone and broadband noise measurements, the sampling rates obtained were 25 kHz and 45 kHz, respectively.

It is important to notice that these results were achieved for a large value of μ (convergence time below 1 s). Therefore, better results could also be obtained with lower values of this parameter (at the expense of a slower convergence time).

The filters obtained in the off-line training step can be seen in Figures 18 and 19. It is essential to notice that the delays posed by the peak of the impulsive response, which represents that time it takes for the signal to pass the secondary path, are close for both filters (taking the different sampling rates into account).

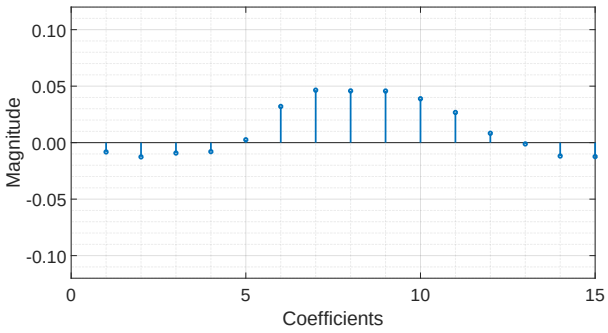

Figure 18: Coefficient values of the 15 taps filter obtained in the off-line training.

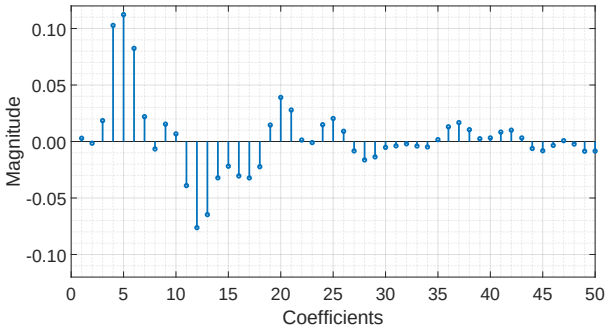

Figure 19: Coefficient values of the 50 taps filter obtained in the off-line training.

The comparison between the filter's frequency response and the headphone measured curve pondered by the simulation of the filters (all normalized by the greatest value) can be seen in Figure 20. The smaller filter, although had a low-pass format, did not represent well the frequencies' variation of the secondary path. The filter with 50 coefficients provided better results in the frequency characterization, but it is still far from the expected curve.

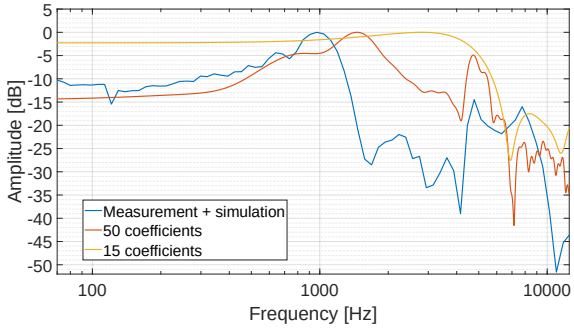

Figure 20: Comparison of both estimations in the frequency domain with the real frequency response of the secondary path.

[3] There are several active noise control algorithms based on neural networks or wavelet transforms. They would be more suitable to be used in nonlinear systems.

However, according to Kuo and Morgan [6], the response of the estimated secondary path does not need to be close to the real one (in the frequency domain). The convergence and effectiveness of the algorithm are not affected significantly by variations in the frequency domain. The most critical information of the estimation is the delay (in samples) provided by the path.

According to some measurements performed by Brent Butterworth [17], commercial headphones with active noise control (ANC) can reach 20 dB to 25dB of reduction in a frequency range from 20 Hz to about 800 Hz (for broadband noise). Therefore, several improvements must be realized to the systems presented within this paper, so they can accomplish similar results as commercial noise-canceling headphones.

7. Discussions and Conclusions

Although these systems are still far from achieving the same reduction as the commercial solutions, satisfactory results were obtained for both noise tests: tonal and wideband. For the tonal noise, the analog system proved to be substantially less effective in comparison to the digital system. Furthermore, the performance of the analog control circuit proved to be more vulnerable to nonlinear situations. The measurements have shown that the broadband noise reduction for the analog system is more centered in higher frequencies than for the digital system.

Better results may be reached with further developments of the circuitry as well as with the correct adjustments of the filter's size and the value of the step size for the digital system.

In addition, the problem regarding the bad coupling between the headphone and the measuring instrumentation may be solved by changing the headphone model or obtaining a smaller artificial ear (for the head and torso simulator). Further studies on the development of algorithms that are more suitable for nonlinear situations are still in development.

References

[1] Elliott, S. and Nelson, P. (1993). Active noise control. IEEE Signal Processing Magazine, 10(4), pp. 12-35.

[2] Kuo, S. and Morgan, D. (1999). Active noise control: a tutorial review. Proceedings of the IEEE, 87(6), pp. 943-975.

[3] Olson, H. and May, E. (1953). Electronic Sound Absorber. The Journal of the Acoustical Society of America, 25(6), pp. 1130-1136.

[4] Clarkson, P. (1993). Optimal and adaptive signal processing. Boca Raton, FL: CRC Press.

[5] Oppenheim, A. and Schafer, R. (2010). Discrete-time signal processing. Upper Saddle River, NJ: Prentice-Hall.

[6] Kuo, S. and Morgan, D. (1996). Active Noise Control Systems: Algorithms and DSP Implementation. New York: Wiley.

[7] Apolinário Jr, J. (2009). QRD-RLS adaptive filtering. New York: Springer.

[8] JLI Electronics. Omnidirectional Back Electret Condenser microphone Cartridge JLI-61A (Datasheet). Available at: `http://bit.ly/JLI61A`. Accessed Jan. 2018.

[9] Fonseca, W. D'A., Zorzo, A., Mareze, P. and Brandão, E. (2018). Audio Signal Conditioning Circuits for Arduino Platforms. In: *DAGA 2018, Meeting of the German Acoustical Society.* Munich, Germany.

[10] Collinson, A. (2017). Op-Amp Microphone Preamp. Available at: `http://bit.ly/OpAmp-Collinson`. Accessed Mar. 2018.

[11] Stoffregen, P. J. and Coon, R. C. PJRCs: Teensy USB Development Board. (2017). Available at: `http://bit.ly/Teensy36`. Accessed Mar. 2018.

[12] Shin K. and Hammond J. (2008). Fundamentals of signal processing for sound and vibration engineers. England: John Wiley & Sons.

[13] Borwick, J. (2001). Loudspeaker and Headphone Handbook. Oxford: Wright.

[14] Analog Devices. AD8606 - Precision, Low Noise, CMOS, Rail-to-Rail, Input/Output Operational Amplifiers (Datasheet Rev. O). Available at: `http://bit.ly/AD8606-AnDev`. Accessed Mar. 2018.

[15] Brüel & Kjær. Head and Torso Simulator (HATS) Type 4128. Available at: `http://bit.ly/BeK-HATS`. Accessed Mar. 2018.

[16] Vafaei, S., Henney, M. and Lamontagne, J. (2016). AKG K44 Headphone Review (rtings.com) Available at: `http://bit.ly/AKGK44-Review`. Accessed Mar. 2018.

[17] Butterworth, B. (2018). Review and Measurements: Bose QC25 Noise-Cancelling Headphone. Available at: `http://bit.ly/QC25Review`. Accessed Mar. 2018.